Biomedical Engineering Letters (2018) 8:127–136
https://doi.org/10.1007/s13534-017-0054-z

ORIGINAL ARTICLE

First demonstration of velocity selective recording from the pig vagus using a nerve cuff shows respiration afferents

B. W. Metcalfe[1] · T. N. Nielsen[2] · N. de N. Donaldson[3] · A. J. Hunter[4] · J. T. Taylor[1]

Received: 1 September 2017 / Revised: 2 November 2017 / Accepted: 15 November 2017 / Published online: 22 November 2017

Abstract
Neural interfaces have great potential to treat disease and disability by modulating the electrical signals within the nervous system. However, whilst neural stimulation is a well-established technique, current neural interfaces are limited by poor recording ability. Low signal amplitudes necessitate the use of highly invasive techniques that divide or penetrate the nerve, and as such are unsuitable for chronic implantation. In this paper, we present the first application of the velocity selective recording technique to the detection of respiration activity in the vagus nerve, which is involved with treatments for epilepsy, depression, and rheumatoid arthritis. Further, we show this using a chronically implantable interface that does not divide the nerve. We also validate our recording setup using electrical stimulation and we present an analysis of the recorded signal amplitudes. The recording interface was formed from a cuff containing ten electrodes implanted around the intact right vagus nerve of a Danish Landrace pig. Nine differential amplifiers were connected to adjacent electrodes, and the resulting signals were processed to discriminate neural activity based on conduction velocity. Despite the average single channel signal-to-noise ratio of − 5.8 dB, it was possible to observe distinct action potentials travelling in both directions along the nerve. Further, contrary to expectation given the low signal-to-noise ratio, we have shown that it was possible to identify afferent neural activity that encoded respiration. The significance of this is the demonstration of a chronically implantable method for neural recording, a result that will transform the capabilities of future neuroprostheses.

Keywords ENG · VSR · Neural interface · MEC · CAP

1 Introduction

Despite the many potential applications of *velocity selective recording* (VSR), it has, until recently, only been demonstrated using the electrically evoked *electroneurogram* (ENG), i.e. *compound action potentials* (CAPs) in *frog* and *pig* [1, 2]. The first application of VSR to naturally occurring (physiological) ENG was made in *rat* using hook electrodes, where afferent activity was detected in the velocity spectrum [3]. These recordings demonstrated two important concepts; firstly, that it is possible to discern naturally occurring spikes using a very simple recording array and basic signal processing and, secondly, that by using a modified VSR process it is possible to extract firing rates for neurons in narrow bands of velocity from the composite recordings in real time. However, a key limitation of this earlier work is the use of hook electrodes, which are not implantable. Hooks were chosen for the experiments in *rat* because they are convenient in acute experiments. They often provide a substantially higher *signal-to-noise ratio* (SNR) than chronically implantable electrode cuffs [3].

In this paper, we present new results from a study that represents the next logical step for VSR development: the first experimental demonstration of VSR using a chronically implantable electrode structure in vivo. Experiments were performed to obtain both electrically

✉ B. W. Metcalfe
b.w.metcalfe@bath.ac.uk

[1] Department of Electronic and Electrical Engineering, University of Bath, Bath, England, UK

[2] Department of Health Science and Technology, Aalborg Universitet, Aalborg, Denmark

[3] Department of Medical Physics and Bioengineering, University College London, London, England, UK

[4] Department of Mechanical Engineering, University of Bath, Bath, England, UK

evoked and physiological ENG from the entire right vagus nerve of an adult female *pig*. The *cervical vagus nerves* (consisting of the left and right) are the tenth pair of cranial nerves and innervate the heart, lungs, upper digestive tract, and other organs of the chest and abdomen. The vagus nerve has become a target of interest for potential neuroprostheses, and vagus nerve stimulation has become an established therapy for patients with disorders such as epilepsy [4], depression [5] and rheumatoid arthritis [6]. The efficacy of vagus nerve stimulation used as a treatment does, however, remain modest as limitations on recording ability have so far precluded the possibility of a closed-loop stimulator that operates on demand. Importantly, it has been demonstrated that the *ensemble* activity recorded from the vagus nerve using a simple nerve cuff can provide a method of early detection of epileptic seizures [7], as well as a respiratory marker [8].

Two sets of experiments were performed in the present study, both using a *multiple electrode cuff* (MEC) for recording. The first experiment used a small *tripolar* cuff for stimulation and a ten-electrode MEC for recording the resulting electrically evoked ENG. The second experiment recorded physiological ENG from the pig at rest, and modulation of the physiological neural signals resulted only from the natural variations in cardiac function, respiration, and blood pressure. Results are presented from both experiments and illustrate the successful stimulation of and recording from the entire vagus nerve using the two cuffs. The experimental setup was the same in both cases.

2 Materials and methods

2.1 Animal preparation

All animal procedures were performed in accordance with the *Danish Animal Experiments Inspectorate* (approval no. 2013-15-2934-00753), as well as the care and use of laboratory animals as described by the *US National Institutes of Health*. In the experiment, an adult female Danish Landrace pig (weight: approximately 50 kg) was sedated with zoletil administered by the *intramuscular* route, transported to the hospital, and then intubated and anaesthetized with sevoflurane and zoletil, also administered intramuscularly. The animal was mechanically ventilated at 15 cycles per minute. An incision of approximately 20 cm was made on the right side of the trachea to expose the right cervical vagus nerve (the tenth cranial nerve), and a section of approximately 15 cm of the nerve was freed from surrounding tissues. The MEC was placed around the nerve at the caudal end of the freed nerve section, while a stimulation cuff was placed on the nerve at the cranial end.

The animal was grounded electrically via a subcutaneous stainless-steel probe, approximately 20 cm in length and 1 cm in diameter, inserted at the abdomen. This ground was also connected to the recording amplifiers. The *electrocardiogram* (ECG) and the vascular blood pressure were recorded independently of the ENG to monitor vital signs. After all surgical procedures had been completed, the anaesthesia was switched to a mixture of ketamine, midazolam, and fentanyl (administered *intravenously*) and the animal was left to stabilise for at least 20 min before performing the experiments. The animal was euthanized after completion of the experiments by an overdose of pentobarbitone.

2.2 Electrode and amplifier configuration

Both the electrode cuffs were produced according to the technique described by Haugland [9]. The stimulation cuff was approximately 12 mm long, with an inner diameter of 2.4 mm, and contained three 1 mm wide platinum-iridium ring electrodes with 5 mm centre-to-centre electrode pitch. The recording cuff was approximately 42 mm long, with an inner diameter of 2.4 mm, and contained ten 1 mm wide ring electrodes with 3.5 mm pitch. The cuffs were placed around the nerve by placing the cuff under the nerve, opening a slit on one side of the cuff, pushing the nerve through, and closing the cuff again. In order to minimize current leakage through the slit, a silicone sheet was placed around the cuff with the opening in the reverse position, and the cuff was closed with ligatures at each end and at the centre. The recording cuff was connected to a custom-made amplifier bank in a *bipolar* configuration and bandpass filtered from 100 Hz to 10 kHz. The overall amplifier voltage gain was 94 dB. In contrast to hook electrodes, the expected amplitudes of the extracellular potentials (V_{ex}) recorded with an MEC are substantially lower (typically, using cuffs, 1–10 μV for physiological ENG and 10–100 μV for CAPs). The amplified and filtered signal was passed to a set of high-speed successive-approximation *analogue to digital converters* (ADCs) (NI9222 mounted in cDAQ-9178 by National Instruments, Austin, TX, USA) providing simultaneous sampling of all ten bipolar recordings at a sample rate of 100 kS/s with 16-bit resolution. The high sampling rate (approximately 10 times the Nyquist frequency for the accepted signal bandwidth of 10 kHz) was necessitated due to the small propagation delays of the faster action potentials, as low as 175 μs. The digitisation range was ± 12 V.

2.3 Velocity selective recording

The essence of VSR is a fundamental process called *delay-and-add* analogous to the delay-and-sum beam-forming algorithms used in many types of synthetic aperture arrays in radar and sonar systems [10]. Each bipolar recording V_{Bi} is delayed relative to the end recording by an interval that depends on both the electrode spacing and the propagation velocity of the signal. So, if the delay inserted between the first two channels (V_{B1}, V_{B2}) is dt then the delay inserted between the first and third channels (V_{B1}, V_{B3}) is 2 dt and so on. The general index of this process is i and $1 \leq i \leq C$ where $C{\cdot}dt$ is the maximum delay of interest. The delay-and-add process essentially operates by cancelling out the naturally occurring delays, after which the channels' outputs are summed, resulting in:

$$V_D[n, dt] = \sum_{i=1}^{C} V_{Bi}[n - (i-1) \cdot dt] \quad (1)$$

where C is the number of recording channels and n is the current sample index [2]. There are two key advantages of the VSR process. Firstly, by using both positive and negative values for dt it is possible to isolate *afferent* and *efferent* neural activity. Secondly, when delay-and-add is used, and the noise sources are uncorrelated (a reasonable assumption), then there is an increase in effective SNR of approximately $\sqrt{C}$ [11]. This property can be exploited to identify neural activity that may not be directly observable in the time records of the individual bipolar channels, and thus could not be detected or classified by traditional spike sorting methods. It is this property for increasing the effective SNR that is exploited in this paper to demonstrate the recording of physiological activity with a chronically implantable (i.e. an MEC) electrode array. For the nine channels of bipolar data, the delay-and-add process should provide an SNR improvement of around three times the original. All data processing was performed offline using standard MATLAB toolboxes, however, the signal processing described in Eq. (1) could easily be performed in real time using an embedded microcontroller.

2.4 Method for extracting respiration

The VSR process can be further extended to extract the firing rates (or *spike trains*), using a signal analysis technique [*velocity spectral density* (VSD)] that has been described previously [3]. This technique produces spike trains with a marker that indicates an action potential with a specific conduction velocity has been detected. In this study we apply the VSD technique in order to extract action potentials that encode afferent respiration information. In order to apply the VSD technique, we extract three different respiration waveforms.

Firstly, a baseline respiration waveform is constructed from the recording of the arterial blood pressure. There is a well-known relationship between blood pressure and respiration, which is proportional to changes in intrathoracic pressure during inspiration and expiration, a summary of which is available in [12].

Secondly, the raw time domain ENG data is segmented and a 20 second window of data is taken from all nine channels, each channel is then bandpass filtered using a 6th order Butterworth IIR filter with cut-off frequencies of 250 Hz and 10 kHz respectively. Further, each channel also has DC offsets and common mode artefacts removed. The common mode artefacts are replaced by null samples over a range of ± 160 μs from the centre of the artefact. After filtering, each channel of ENG is smoothed using a sliding RMS window of length 500 ms. The result of this process is an RMS waveform that illustrates the level of neural activity within the entire nerve.

The final stage of the analysis process is to distinguish between afferent and efferent activity, as well as to identify the individual action potentials and classify them based on conduction velocity. The raw ENG is filtered in the manner described previously, but without the RMS smoothing being applied. The VSD method can then be applied to extract the individual action potentials [3].

3 Results

3.1 Electrically evoked data

Electrical stimulation was applied to the nerve using the tripolar stimulation cuff, the purpose of this was to both validate the recording setup and determine the range of velocities that might be supported by the nerve. The stimulation profile consisted of charge-balanced square pulses, with a primary cathodic phase of 100 μs duration and amplitude ranging from 0 to 5 mA in steps of 100 μA, followed, after a delay of 100 μs, by an anodic phase of 2 ms duration and 5% of the cathodic amplitude, which was repeated ten times. Figure 1 illustrates the composite time domain recording made by averaging ten stimulation events that were at the maximum stimulus of 5 mA, and clearly indicates two *electrically evoked compound action potentials* (eCAPs). The leftmost marker represents the stimulation artefact and the two successive markers represent the two dominant eCAPs with conduction velocities of approximately 58 and 15 m/s and peak amplitudes of 200 and 10 μV respectively. The recording cuff was located approximately 5 cm caudally from the stimulation

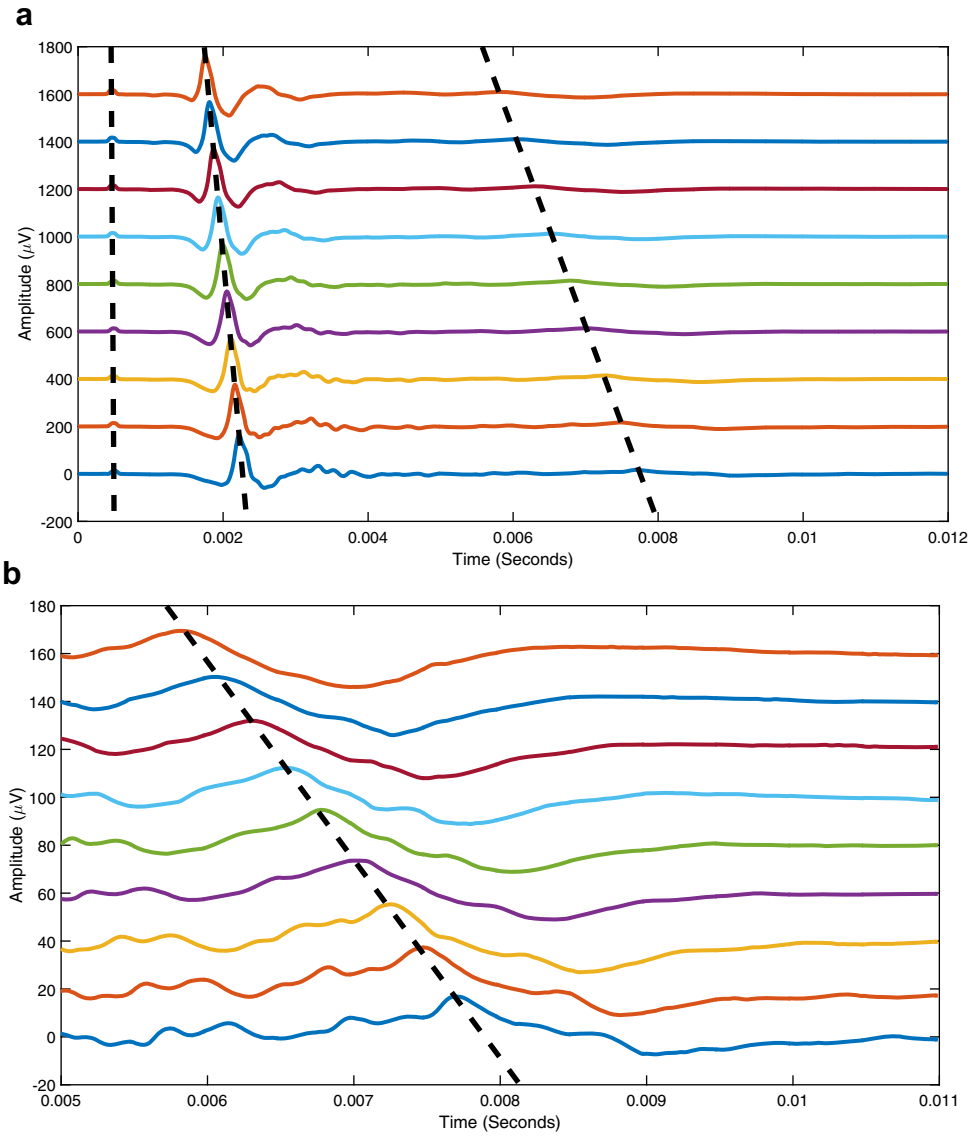

Fig. 1 **a** Composite time domain recording for a maximal stimulation event. Each trace is the average of ten stimulation events, the first marker indicates the stimulation artefact, with successive markers indicating the two dominant eCAPs at 58 and 15 m/s respectively. **b** Zoomed section from **a** that illustrates the slower eCAP occurring approximately 6 ms after the stimulation event. Note the reduced amplitude corresponding to the approximate square law relationship between velocity and amplitude for myelinated axons

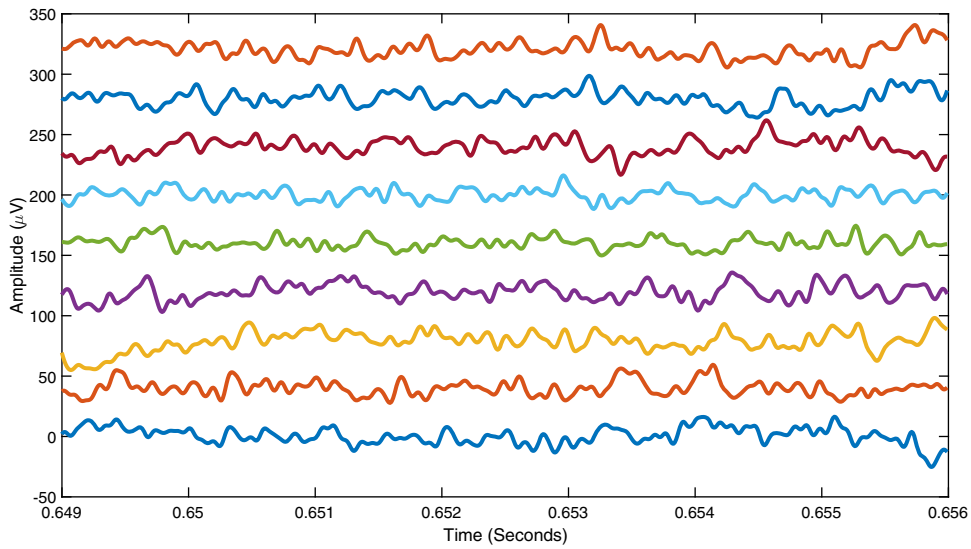

Fig. 2 Time domain recording of physiological ENG from the right cervical vagus nerve, there are few visually discernible features that could be attributable to ENG activity. The ordinate is input-referred signal (voltage), the offsets have been added artificially for presentation purposes. The raw data have been bandpass filtered with an 8th order Butterworth digital filter between 250 Hz and 10 kHz. The RMS amplitude for the data, averaged over all nine channels, is 19.5 μV

cuff. The offset in the data has been added artificially for the purposes of presentation.

The slower eCAP has a markedly lower amplitude compared to the faster one. The well-known reason for this is that, for myelinated axons, there is an approximately square law relationship between conduction velocity and amplitude, both being a function of the axon diameter [13]. Indeed, the velocity ratio of the two populations is approximately 4:1, which—using a square law relationship—would result in an amplitude ratio of 16:1; the measured ratio is approximately 20:1. However, this calculation would only be exactly true if the two populations of fibres each had the same velocity, the same number of fibres, and all fired simultaneously, which will not be true.

The electrically evoked data validate the recording configuration and provide a measure of the types of axons that were present within the nerve, namely those in the range of conduction velocities from 15 to 58 m/s corresponding predominantly to the Aδ and Aβ fibre types respectively. These axons are most likely responsible for baroreceptors in the lungs and heart, as well as parasympathetic efferent fibres innervating the heart, and possibly laryngeal motor fibres. The vagus nerve also contains many C fibres, which are unmyelinated and with conduction velocities below 5 m/s. These are not seen in the eCAP recording probably due to the very low action potential amplitude associated with the square law.

3.2 Naturally occurring neural activity

After the electrically evoked data was recorded, the animal was left to stabilise for a period of 2 min before bipolar recordings of naturally occurring (or physiological) ENG were made using the same recording setup. These recordings were made with the animal at rest; no artificial stimulation was applied either electrically or mechanically. As with the electrical stimulation, a continuous recording was made that lasted 2 min, the data was sampled concurrently over all nine bipolar channels at a sample rate of 100 kS/s with 16-bit resolution. The raw data contained several interference artefacts that appeared as common mode signals in all channels and appeared periodically at a rate of approximately two per second, each artefact was a short burst of oscillations with a frequency of approximately 15 kHz. A 7 ms segment of the time domain data without interference artefacts is shown in Fig. 2. Within the time domain recordings of the physiologically ENG, there are few (if any) visually discernible features that could be attributable to neural activity. As with the electrically evoked recordings, the ordinate scale in each case represents the signal voltage after application of 94 dB voltage gain and the offsets have been added artificially for presentation purposes. Channel one (top trace) is cranial and channel nine (bottom trace) is caudal. The raw data have been bandpass filtered with an 8th order Butterworth digital filter between 250 Hz and 10 kHz in post-processing.

The delay-and-add approach was applied to the short time segment of Fig. 2 over the range of conduction velocities from 31 to 45 m/s in steps of 2 m/s. These limits were chosen after first exploring wider limits (5–80 m/s) and identifying the range of values that produced the largest responses. The step size of 2 m/s in this instance was chosen for presentation reasons. The result of the delay-and-add process of Eq. (1) is shown in Fig. 3, where each waveform is the result of adding together all the nine bipolar time domain recordings with a delay factor $\tau = d/v$ corresponding to each velocity. Clearly visible within the data are correlated peaks that reveal action potentials with conduction velocities in the chosen range.

3.3 Statistical analysis

To quantify the significance of the peaks in Fig. 3, a statistical analysis was performed that relies on the assumption that the noise sources in the raw data consist of uncorrelated *additive white Gaussian noise* (AWGN). Firstly, the standard deviations for each of the nine raw data channels were calculated using conventional methods. These standard deviations were then summed to produce the expected standard deviation σ_{sum} after the delay-and-add process assuming only noise in the original recordings:

$$\sigma_{sum} = \sqrt{\sigma_1 + \sigma_2 + \cdots + \sigma_9} \quad (2)$$

Thus, if each of the nine raw data channels contained purely uncorrelated AWGN then the expected standard deviation after summing all channels together is σ_{sum}, which was found to have a value of 19.4 μV. This value was used to construct a confidence threshold of 3σ variation from the mean of 58.4 μV. This threshold is indicated in Fig. 3 as the two dashed lines located at ± 58.4 μV. Any values for Eq. (1) that lie outside this range are hypothesised to be the result of correlated events between the raw data channels, i.e. naturally occurring action potentials. In Fig. 3, there are seven such events with positive amplitude and two with negative amplitude. The approximate peak delay (and thus velocity) for the events are given in Table 1.

3.4 Extraction of respiration

The analysis methods described previously were applied to the naturally occurring data in order to extract action potentials that encode respiration. Firstly, the baseline respiration signal was extracted from the blood pressure waveform. Figure 4a illustrates the time domain recording of the arterial blood pressure (non-calibrated, relative

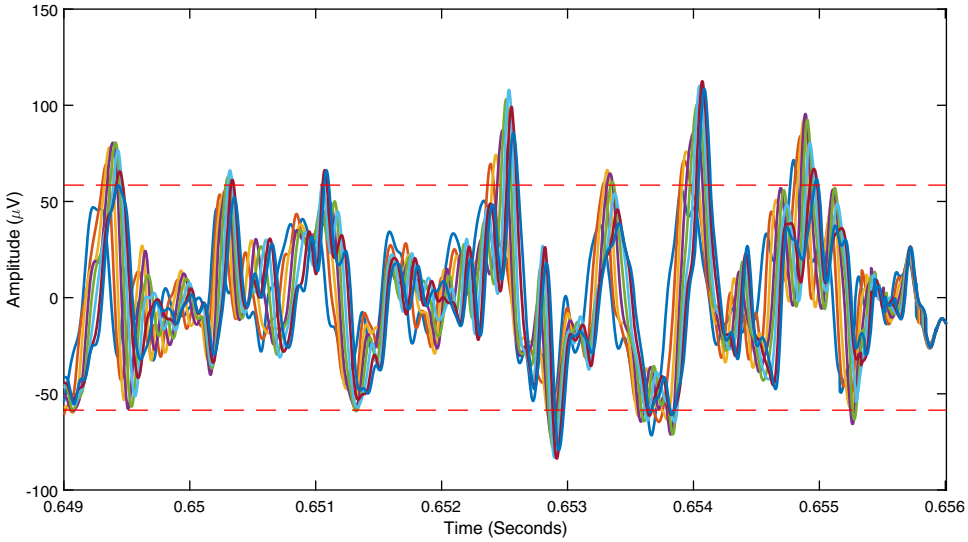

Fig. 3 The post delay-and-add (beam formed) waveforms for the physiological recording of Fig. 2 for conduction velocities in the range 31–45 m/s with an interval of 2 m/s, correlated peaks are clearly visible revealing efferent action potentials that are not discernible in Fig. 2. The dashed thresholds represent $\pm 3\sigma$ deviation from the mean assuming purely uncorrelated AWGN sources (absolute value = 58.4 μV)

Table 1 Approximate conduction velocities and peak amplitudes for the correlated events that exceed the positive 3σ threshold in Fig. 3

Event	Approximate velocity (m/s)	Peak amplitude (μV)
1	37	80.51
2	41	66.04
3	44	66.15
4	41	107.70
5	44	− 83.62
6	35	66.08
7	42	112.40
8	43	95.45
9	37	− 65.63

values only) recorded from a catheter within the Carotid artery. There is a clear modulation of the blood pressure by the action of respiration, as shown by the variation in the envelope of the blood pressure, this respiration signal has been extracted and is shown in the dashed line. The extracted respiration rate is approximately 0.25 Hz, which agrees with prescribed ventilator rate of 15 cycles per minute.

Secondly, the RMS smoothing technique was applied to the raw ENG, and the results are shown in Fig. 4b. There is a clear correlation between the increase in overall signal amplitude of the ENG with the respiration signal extracted from the arterial blood pressure. This result indicates that there is a large number of axons within the right vagus nerve related to respiration.

Finally, the VSD analysis technique was applied to the data in order to extract individual action potentials. Throughout this process an overall VSD detector threshold was set at 10 dB (relative to the median signal value after the delay-and-add process), this is equal to an absolute voltage threshold of approximately 45 μV. The results of the VSD analysis are shown in Fig. 4c for afferent activity and Fig. 4d for efferent activity. The afferent spike patterns extracted for conduction velocities between 20 and 70 m/s demonstrate clear correlation between activity centred about 30–40 m/s and the respiration waveform. The total number of spikes above threshold (10 dB to the median) was 2254. The efferent spike patterns extracted for conduction velocities between − 20 and − 70 m/s demonstrate no obvious visual correlation between activity and the respiration or blood pressure waveform. The total number of spikes above threshold (10 dB to the median) was 1440.

In order to examine the correlation, the extracted spikes were segmented based on conduction velocity into Aβ (33–75 m/s) and Aδ (3–30 m/s), for the both efferent and afferent cases. The segmented spikes were then converted into a time domain waveform by the following process: Firstly, the single sample spike events were convolved with a 500 ms sliding Gaussian window. Secondly, the resulting activity waveform was low-pass filtered at 0.5 Hz with a 4th order Butterworth IIR filter. Finally, both the respiration waveform and the segmented spike waveforms were normalised to their own standard deviations for comparison. The resulting waveforms are shown in Fig. 5 for the case of the afferent Aβ fibres, Table 2 shows the correlation coefficients and the lag in seconds at which that correlation occurred for all of the extracted waveforms.

4 Discussion

The results for the electrical stimulation experiment demonstrate that the interface could record eCAPs throughout the duration of the experiment, with good levels

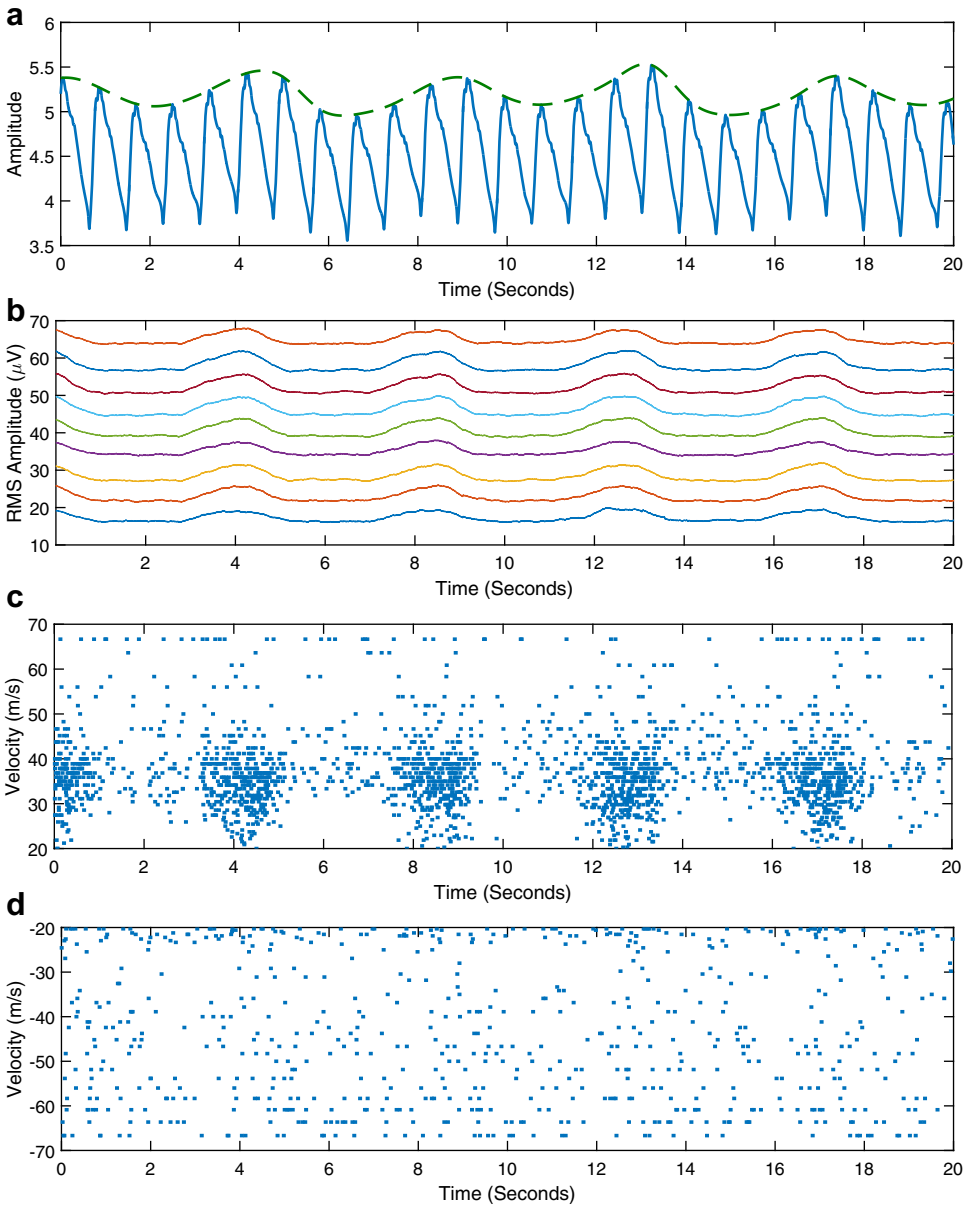

Fig. 4 **a** The time domain recording of the arterial blood pressure (non-calibrated) recorded from a catheter within the Carotid artery is shown in the solid trace. There is a clear modulation of the blood pressure by the action of respiration, and a respiration signal has been extracted by fitting an envelope to the blood pressure waveform (dashed line). The respiration rate is 0.25 Hz. **b** The time domain recording of the raw ENG over all nine channels. Each channel has been filtered using a bandpass filter with cut-off frequencies of 250 Hz and 10 kHz respectively, DC offsets have been removed and a common mode rejection algorithm has been applied. Further, each channel has then been averaged using a rolling RMS window of length 500 ms. Clearly visible in each channel is an increase in overall signal amplitude that is correlated to the respiration waveform of **a**. **c** The *afferent* spike pattern extracted for conduction velocities between 20 and 70 m/s, each marker indicates a spike. The total number of spikes above threshold (10 dB to the median) was 2254. There is a clear correlation between afferent activity centred about 30–40 m/s and the respiration waveform. **d** The *efferent* spike pattern extracted for conduction velocities between − 20 and − 70 m/s, each marker indicates a spike. The total number of spikes above threshold (10 dB to the median) was 1440. There is no obvious correlation between efferent activity and the respiration or blood pressure waveform

of SNR and a range of conduction velocities from 15 to 58 m/s, corresponding predominantly to the Aδ and Aβ fibre types respectively. There were only two main eCAP events identified within the time domain recordings, however, it was expected that the cervical vagus would also contain C fibres that, if they were being stimulated, would have had a response that was too small to be detectable. Indeed, the recording of C fibre activity from a large nerve represents one of the key remaining challenges of current neural recording systems.

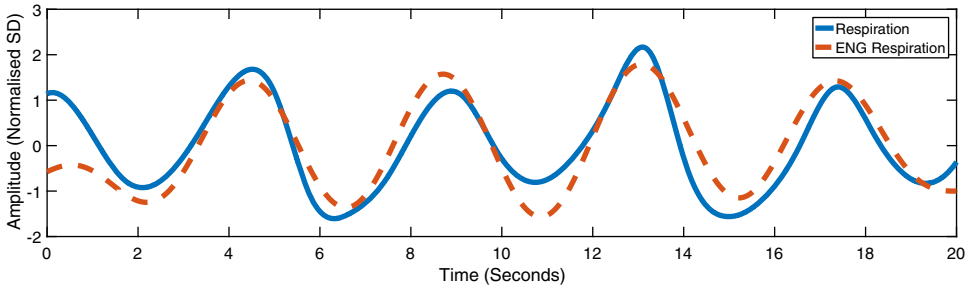

Fig. 5 The respiration signal extracted from Fig. 4a is plotted alongside the Aβ *afferent* activity extracted from the vagus nerve. In order to transform the spike patterns from Fig. 4c a 500 ms Gaussian window was convolved with the spikes in the Aβ range, and the resulting waveform was then low-pass filtered at 0.5 Hz with a 4th order Butterworth digital filter. Both signals were normalised to their own standard deviations for comparison

Table 2 Correlation coefficients and lags for the extracted signals relative to the baseline respiration waveform

Signal	Correlation coefficient	Lag (s)
RMS smoothed ENG	0.69	− 0.443
Aβ afferent	0.72	0.036
Aδ afferent	0.69	0.023
Aβ efferent	0.23	− 12.969
Aδ efferent	0.50	− 2.328

The recording of physiological ENG was performed with the same recording setup as the electrical stimulation experiment, with no change at all in the configuration. It was not possible to directly observe individual action potentials within the dipole recordings, which is the familiar situation with recording cuffs: their internal resistance is too low for the action current to generate a potential that is distinguishable from the noise.

The application of the standard delay-and-add process, which should yield an improvement in SNR of about three ($\sqrt{N}$ where $N = 9$ in this case), produces a result with clear and distinct peaks, as shown in Fig. 3. These peaks exhibit a clear relationship that is a direct result of inter-channel correlation, namely that the amplitude of the waveforms is directly proportional to artificial delay that is applied. Furthermore, when the statistical properties of the noise are examined, and the total expected variance from the mean is computed, it has been shown that multiple events exist (post delay-and-add) that are beyond the 3σ significance threshold. These events correlate with a delay that is suggestive of a conduction velocity well within the expected range, and within the range demonstrated using electrical stimulation.

However, as shown in Table 1, the peaks obtained after delay-and-add are about 90 μV, or, on average, 10 μV per dipole. This is a surprisingly large value that meant that we treated these results with caution. In [14] we presented a physical model of an axon in a cuff and derived the recorded action potential from the *trans-membrane action potential* (TMAP), the electrode pitch, the propagation velocity, the cuff radius and the resistivities of axoplasm and the volume conductor within the cuff. For a dipole, the recorded potential function is

$$V_{dp}(t, z_1, z_2) = \left(\frac{\rho_\epsilon}{\rho_\alpha}\right)\left(\frac{r_a}{r_e}\right)^2 \left[V_m\left(t - \frac{z_1}{v}\right) - V_m\left(t - \frac{z_2}{v}\right)\right] \tag{3}$$

where z_1 and z_2 are the electrode positions, ρ_e and ρ_a are the resistivities of the tissue inside the cuff and of the axoplasm respectively, r_e and r_a are the internal radii of the cuff and the axon, V_m is the transmembrane action potential, and v is the conduction velocity. For the cuff in this experiment, the 3.5 mm pitch was large enough that even at 70 m/s the peak value of the expression in the square brackets is close to the peak value of the TMAP ($\sim$ 60 mV). If the bore of the 70 m/s fibre is 7 μm and of the cuff was 2.4 mm, the peak value of V_{dp} would be 0.5 μV multiplied by $(\rho_\epsilon/\rho_\alpha)$. So, to get 10 μV, this quotient would need to be approximately 20. This is not perhaps impossible for a snug-fitting cuff before the growth of encapsulation tissue, where typical values might be $\rho_e = 1.1$ kΩ cm and $\rho_a = 70$ Ω cm [15, 16]. Unfortunately, no impedance measurements were made during the experiment that could have shown this to be the case. At 20 m/s, the equivalent amplitude multiplier is 0.04 μV, so the recorded action potentials would be more than ten times smaller.

Figure 4a–d shows the correlation between the afferent action potentials and the independently-recorded respiration. This is convincing evidence that action potential velocities can be detected using the VSD method, not only from microchannels [17] but sometimes, as in this experiment, from cuffs on whole nerves, if the internal resistance of the cuff is high. The conduction velocities that are most strongly correlated to respiration are in the range expected for both the Aδ and Aβ sensory axons, although the

analysis was restricted to only the top end of the Aδ conduction range. There is significantly less, if any, correlation between respiration and efferent activity in either the Aδ or the Aβ conduction ranges.

The lag values given in Table 2 should be treated with some caution. Whilst the RMS process introduces a lag in the smoothed ENG, it is also likely that any earlier rise in activity is during the expansion of the lungs and before the effect of modulation on the blood pressure. There are most likely two factors that make a direct timing analysis problematic: firstly, it is difficult to make conclusions about what to expect in terms of efferent or afferent activity, considering that the animal was artificially ventilated. It is likely that the natural respiration drives were not entirely surpressed, although may become reset or adjusted to the artificial ventilation rate. Secondly, because the respiration waveform has been extracted from the blood pressure, there will be an unknown time delay between changes in intrathoracic pressure and changes in the blood pressure.

One question that arises from these results is why the eCAP appears to give two distinct populations of axons in the nerve whereas the spike patterns show a broad spread of velocities from + 70 to − 70 m/s, excluding the slow range from + 20 to − 20 m/s. Part of the answer is probably that many of the axons that were activated in the eCAP were quiescent during the natural activity, so that the distribution of active fibres is different in the two situations. Nevertheless, it is strange that such a sharp peak at 58 m/s in Fig. 1 should not have any significant corresponding activity in Fig. 4, either in the afferent or efferent direction. This question will need further examination, a potential explanation could be that these are laryngeal fibres which may be inactive due to the sedation of the animal.

5 Conclusions

This study has, for the first time, demonstrated the application of the *velocity selective recording* technique to the recording of both electrically evoked and physiological neural signals from the cervical vagus nerve. A simple interface was formed from a *multiple electrode cuff* containing ten recording electrodes, the cuff was implanted on the intact right cervical vagus nerve of an anesthetised Danish landrace pig. The ten channels were amplified and filtered before post-processing was applied to discriminate neural activity based on conduction velocity. As a direct result of the measurements, a surprising discovery has been made: although the single channel signal-to-noise ratio is on the order of − 5.8 dB, it is possible—using the velocity selective recording method—to observe distinct action potentials travelling in both directions along the vagus nerve, with a range of conduction velocities consistent with Aδ and Aβ fibre types. Further, it is possible to automatically extract firing rates, in real time, for each velocity. These firing rates show a clear correlation between respiration and activity within the sensory (afferent) pathways of the vagus nerve.

The outcomes of this study have shown that it is possible to record physiological neural activity, discriminated in both direction and conduction velocity, from large nerves using a chronically implantable, real time technique. Further studies can use this result to drive the development of future neuroprostheses that make use of real time neural recordings.

Compliance with ethical standards

Conflict of interest We wish to declare that we have no commercial affiliations, consultancies, stock or equity interests, or patent-licensing arrangements that could be considered to pose a conflict of interest regarding the submitted manuscript.

Ethical approval All animal procedures were performed in accordance with the Danish Animal Experiments Inspectorate (approval no. 2013-15-2934-00753), as well as the care and use of laboratory animals as described by the U.S National Institutes of Health.

References

1. Schuettler M, Donaldson N, Seetohul V, Taylor J. Fibre-selective recording from the peripheral nerves of frogs using a multi-electrode cuff. J Neural Eng. 2013;10:36016. https://doi.org/10.1088/1741-2560/10/3/036016.
2. Schuettler M, Seetohul V, Rijkhoff NJM, Moeller FV, Donaldson N, Taylor J. Fibre-selective recording from peripheral nerves using a multiple-contact cuff: report on pilot pig experiments. Conf Proc IEEE Eng Med Biol Soc. 2011;2011:3103–6. https://doi.org/10.1109/IEMBS.2011.6090847.
3. Metcalfe BW, Chew DJ, Clarke CT, Donaldson NN, Taylor JT. A new method for spike extraction using velocity selective recording demonstrated with physiological ENG in rat. J Neurosci Methods. 2015;251:47–55. https://doi.org/10.1016/j.jneumeth.2015.05.003.
4. Connor DE, Nixon M, Nanda A, Guthikonda B. Vagal nerve stimulation for the treatment of medically refractory epilepsy: a review of the current literature. Neurosurg Focus. 2012;32:E12. https://doi.org/10.3171/2011.12.FOCUS11328.
5. George MS, Sackeim HA, Rush AJ, Marangell LB, Nahas Z, Husain MM, Lisanby S, Burt T, Goldman J, Ballenger JC. Vagus nerve stimulation: a new tool for brain research and therapy. Biol Psychiatry. 2000;47:287–95. https://doi.org/10.1016/S0006-3223(99)00308-X.
6. Koopman FA, Chavan SS, Miljko S, Grazio S, Sokolovic S, Schuurman PR, Mehta AD, Levine YA, Faltys M, Zitnik R, Tracey KJ, Tak PP. Vagus nerve stimulation inhibits cytokine production and attenuates disease severity in rheumatoid arthritis. Proc Natl Acad Sci USA. 2016;113:8284–9. https://doi.org/10.1073/pnas.1605635113.
7. Nielsen TN, Struijk JJ, Harreby KR, Sevcencu C. Early detection of epileptic seizures in pigs based on vagus nerve activity. In:

Pons JL, Torricelli D, Pajaro M, editors. Converging clinical and engineering research on neurorehabilitation. Berlin: Springer; 2013. p. 43–7.
8. Sevcencu C, Nielsen TN, Kjaergaard B, Struijk JJ. A respiratory marker derived from left vagus nerve signals recorded with implantable cuff electrodes. Neuromodulation Technol Neural Interface. 2017;. https://doi.org/10.1111/ner.12630.
9. Haugland M. A flexible method for fabrication of nerve cuff electrodes. In: Proceedings of 18th annual international conference of the IEEE engineering in medicine and biology society. IEEE; 1996. p 359–360.
10. Huang Y, Miller JP. Phased-array processing for spike discrimination. J Neurophysiol. 2004;92:1944–57. https://doi.org/10.1152/jn.00088.2004.
11. Donaldson N, Rieger R, Schuettler M, Taylor J. Noise and selectivity of velocity-selective multi-electrode nerve cuffs. Med Biol Eng Comput. 2008;46:1005–18. https://doi.org/10.1007/s11517-008-0365-4.
12. Lorenzi-Filho G, Dajani HR, Leung RS, Floras JS, Bradley TD. Entrainment of blood pressure and heart rate oscillations by periodic breathing. Am J Respir Crit Care Med. 1999;159:1147–54. https://doi.org/10.1164/ajrccm.159.4.9806081.
13. Seidl AH. Regulation of conduction time along axons. Neuroscience. 2014;276:126–34. https://doi.org/10.1016/j.neuroscience.2013.06.047.
14. Taylor J, Donaldson N, Winter J. Multiple-electrode nerve cuffs for low-velocity and velocity-selective neural recording. Med Biol Eng Comput. 2004;42:634–43. https://doi.org/10.1007/BF02347545.
15. Grill WM, Mortimer JT. Electrical properties of implant encapsulation tissue. Ann Biomed Eng. 1994;22:23–33. https://doi.org/10.1007/BF02368219.
16. Struijk JJ. The extracellular potential of a myelinated nerve fiber in an unbounded medium and in nerve cuff models. Biophys J. 1997;72:2457–69. https://doi.org/10.1016/S0006-3495(97)78890-8.
17. Chew DJ, Zhu L, Delivopoulos E, Minev IR, Musick KM, Mosse CA, Craggs M, Donaldson N, Lacour SP, McMahon SB, Fawcett JW. A microchannel neuroprosthesis for bladder control after spinal cord injury in rat. Sci Transl Med. 2013;5:210. https://doi.org/10.1126/scitranslmed.3007186.